

Coadsorption of a Polyanion and an Azobenzene Dye in Self-Assembled and Spin-Assembled Polyelectrolyte Multilayers

Victoria E. Campbell,^{†,§} Peter A. Chiarelli,[‡] Sanjit Kaur,[†] and Malkiat S. Johal^{*,†}

*Division of Natural Sciences, New College of Florida, Sarasota, Florida 34243, and
Faculty of Clinical Medicine, Oxford University, Oxford OX1-3JA, U.K.*

Received July 6, 2004. Revised Manuscript Received October 15, 2004

We describe the integration of a photochromic azobenzene dye into electrostatically bound polyelectrolyte multilayers. Two different deposition techniques are compared: electrostatic self-assembly (ESA) and polyelectrolyte spin-assembly. The polyelectrolytes used were PEI (polyethylenimine) and PAZO (poly[1-[4-(3-carboxy-4-hydroxyphenylazo) benzenesulfonamido]-1,2-ethanediyl, sodium salt]). Successful incorporation of the azobenzene dye Direct red 80 (DR80) into ESA and spin-assembled multilayered films (PEI/DR80) is demonstrated. We find that coadsorption of DR80 and PAZO on a PEI surface occur in different proportions and packing densities, depending on the assembly technique selected. We find that using DR80 as a coadsorbing agent can dramatically enhance the rate of PAZO adsorption, and we observe different deposition rates for DR80 and PAZO when the two materials adsorb simultaneously from a common solution.

Introduction

Electrostatic self-assembly (ESA) by the sequential adsorption of polycations and polyanions is now a well-established and versatile method for constructing multilayered films of alternating charge composition near thermodynamic equilibrium.^{1–3} Although commonly used to successively adsorb polymeric materials or macromolecules of opposite charge, ESA is not constrained by the requirement of polyelectrolytes.^{4–7} For example, Rubner has demonstrated charge alternating dye–dye ESA to build multilayered films, suggesting that these monomeric species undergo charge overcompensation during adsorption.⁸

Photochromic materials incorporated into such multilayered films may possess technological benefits in areas such as nonlinear optics, holography, data storage, and organic LED development.^{3,9} Azobenzene derivatives, specifically, are candidates for photochromic materials due in part to their photoisomerization properties. In a recent study, Advincula et al. described photoalignment reversibility in multilayered

films containing the water soluble anionic azobenzene dye direct red 80 (DR80), offering the potential for read–write capabilities.⁶ The ability to integrate multiple photochromic species into a self-assembled thin film, while demonstrating control over molecular architecture and deposition kinetics, is important for the development of functional devices. In this paper, we describe the assembly of thin films composed of the polycation PEI (polyethylenimine) and anionic DR80. We also present the first description of competitive adsorption between anionic DR80 and a polyanion (PAZO, poly[1-[4-(3-carboxy-4-hydroxyphenylazo) benzenesulfonamido]-1,2-ethanediyl, sodium salt]), comparing results from films constructed by the established ESA technique and the new method of spin-assembly.^{10,11} The molecular structures of DR80, PEI, and PAZO are shown in Figure 1.

The self-assembly methods used in this study have been described in previous work.^{12–14} Although conventional ESA typically entails polyelectrolyte deposition of alternating charge, notable exceptions exist where deposition has been observed in the absence of such an alternating scheme.^{15–17} Distinct from ESA, spin-assembly relies on attractive interactions and physical entanglement of molecular subunits to induce adsorption from solutions deposited on a rapidly spinning substrate. Deposition occurs in fractions of a second,

* To whom correspondence should be addressed. E-mail: johal@ncf.edu. Fax: (941) 359-4396.

[†] New College of Florida.

[‡] Oxford University.

[§] Current address: Department of Material Science and Engineering, University of Wisconsin-Madison, 1500 Engineering Dr., Madison, WI 53726.

(1) Decher, G. *Science* **1997**, *277*, 1232.

(2) Decher, G.; Hong, J. D.; Schmit, J. *Thin Solid Films* **1992**, *210/211*, 831.

(3) Tripathy, S. K.; Jayant, K.; Singh, N. H.; MacDiarmin, A. G., Eds.; *Handbook of Polyelectrolytes and Their Applications, Volume 1: Polyelectrolyte-Based Multilayers, Self-Assemblies and Nanostructures*; American Scientific Publishers: Stevenson Ranch, CA, 2002.

(4) Ariga, K.; Lvov, Y.; Kunitake, T. *J. Am. Chem. Soc.* **1997**, *119*, 2224.

(5) Cooper, T.; Campbell, A.; Crane, R. *Langmuir* **1995**, *11*, 2713.

(6) Advincula, R.; Fells, E.; Park, M. *Chem. Mater.* **2001**, *13*, 2870.

(7) Advincula, R.; Park, M.; Baba, A.; Kaneko, F. *Polym. Mater. Sci. Eng.* **1999**, *81*, 77.

(8) Yoo, D.; Wu, A.; Lee, J.; Rubner, M. *Synth. Met.* **1997**, *85*, 1425.

(9) Ichimura, K. In *Polymers as Electrooptical and Photooptical Active Media*; Shibaev, V., Ed.; Springer: Berlin, 1996.

(10) Chiarelli, P. A.; Johal, M. S.; Casson, J. L.; Roberts, J. B.; Robinson, J. M.; Wang, H.-L. *Adv. Mater.* **2001**, *13*, 1167.

(11) Cho, J.; Char, K.; Hong, J. D.; Lee, K. B. *Adv. Mater.* **2001**, *13*, 1076.

(12) Casson, J. L.; McBranch, D. W.; Robinson, J. M.; Wang, H.-L.; Roberts, J. B.; Chiarelli, P. A.; Johal, M. S. *J. Phys. Chem. B.* **2000**, *104*, 11996.

(13) Chiarelli, P. A.; Johal, M. S.; Holmes, D. J.; Casson, J. L.; Roberts, J. B.; Robinson, J. M.; Wang, H.-L. *Langmuir* **2002**, *18*, 168.

(14) Casson, J. L.; Wang, H.-L.; Roberts, J. B.; Parikh, A. N.; Robinson, J. M.; Johal, M. S. *J. Phys. Chem. B.* **2002**, *106*, 1697.

(15) Johal, M. S.; Casson, J. L.; Chiarelli, P. A.; Liu, D.; Shaw, J. A.; Robinson, J. M.; Wang, H.-L. *Langmuir* **2003**, *19*, 8876.

(16) Cho, J.; Caruso, F. *Macromolecules* **2003**, *36*, 2845.

(17) Fischer, P.; Laschewsky, A. *Macromolecules* **2000**, *33*, 1100.

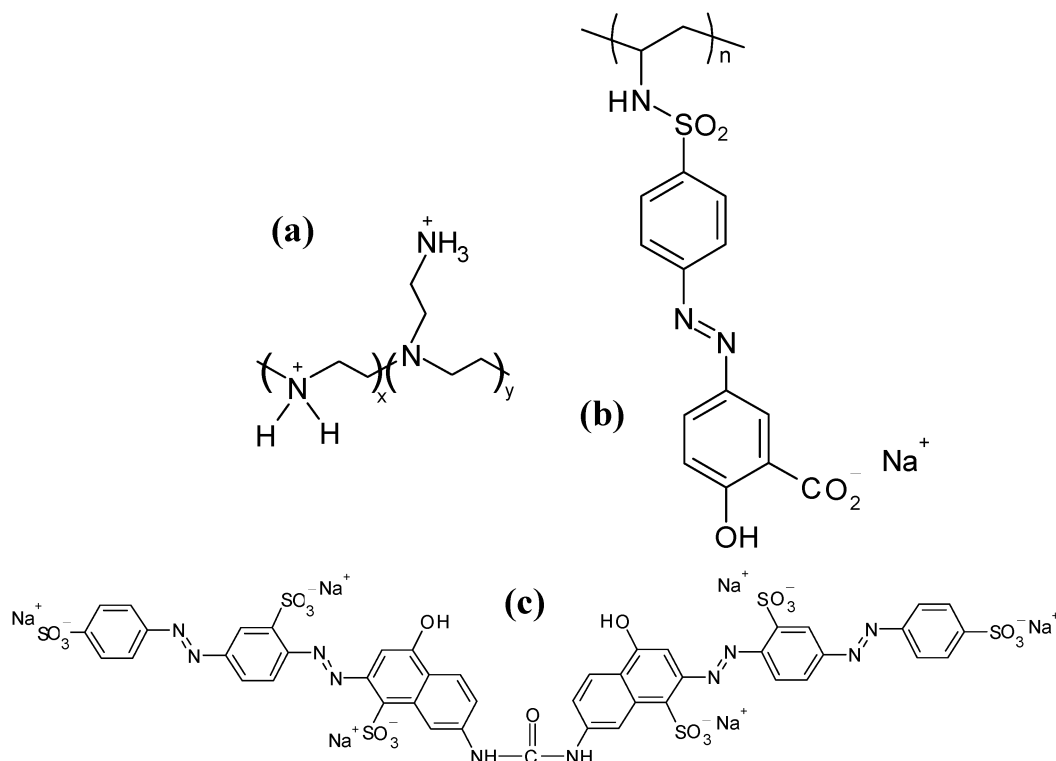


Figure 1. Structures of (a) PEI (polyethylenimine), (b) PAZO (poly[1-[4-(3-carboxy-4-hydroxyphenylazo) benzenesulfonamido]-1,2-ethanediyl, sodium salt]), and (c) DR80 (direct red 80).

and yields highly robust layers of reproducible dimension. Due to the involvement of mechanical entanglement forces in spin-assembly, successful deposition of like-charge materials is achievable in a variety of systems.¹³ Previous studies have shown that Coulombic attraction between polyelectrolyte layers enhances the amount of polyelectrolyte deposited, although the lack of such an attraction does not prevent deposition entirely, as it might in ESA.^{15,17} Thus, significant composition differences may be expected when constructing PEI/DR80 and PEI/(DR80+PAZO) bilayers. In this work we use UV–visible spectroscopy and single-wavelength ellipsometry to show that deposition of DR80 on PEI is significantly influenced by the deposition process chosen, with layers of lower packing density constructed by spin-assembly, compared to ESA. We also demonstrate that coadsorption of DR80 and PAZO on a PEI surface may be influenced to occur in different proportions, depending on the assembly technique selected.

Experimental Section

DR80, PEI (MW = 25 000 g mol⁻¹, mixture of linear and branched chains), and PAZO were obtained from Aldrich and used as received. The degree of protonation determines the charge density of the cationic PEI. Approximately 75% of the amino groups of PEI are protonated at pH 2 with the degree of protonation decreasing linearly to zero charge at pH ~11.¹⁸ The pH of the PEI solutions used in this study was approximately 7. All polyelectrolyte solutions were prepared at 1 mM (based on the molecular weight of the polymer repeat unit), and DR80 was prepared at 0.025 mM using ultrapure water (resistivity >18 MΩcm). Aqueous solutions containing a mixture of 1 mM PAZO and 0.025 mM DR80 were also prepared for the coadsorption studies.

Substrates for film deposition were glass microscope slides for UV–visible spectroscopy measurements, and round 1-in. polished silicon wafers for ellipsometry. The same native oxide outerlayers for all substrate types provided reproducible surface conditions for film deposition. Substrates were prepared by immersion in a 30:70 H₂O₂ (30% weight)/H₂SO₄ (concentrated) mixture for 1 h at 80 °C (piranha etch treatment).¹⁹ This treatment exposes the free silanol (–Si–OH) groups on the substrate surface, which subsequently deprotonate at higher pH conditions (pH >2), resulting in an overall negatively charged surface. Following this treatment, substrates were rinsed thoroughly in water, sonicated for 15 min to remove any remaining etch solution, and then stored in ultrapure water. Prior to film deposition, substrates were rinsed again with water and dried under a stream of nitrogen gas.

For the kinetics measurements, after a single layer of PEI was adsorbed onto a glass substrate, the substrate was immersed for 30 s in either the mixed aqueous PAZO+DR80 solution or the pure aqueous DR80 solution, rinsed with water, and then dried with a stream of nitrogen. UV–visible spectroscopy was used to monitor the amount of PAZO and DR80 adsorbed. After a spectrum was obtained, the glass substrate was re-immersed in the solution for an additional 30 s. This process was repeated until the UV–visible spectra showed no discernible increase in PAZO and/or DR80 adsorption.

Electrostatically self-assembled multilayers were constructed using the following method. Clean substrates were immersed in a PEI solution for five minutes at room temperature, and then rinsed with ultrapure water and dried under a stream of nitrogen gas. The substrate was then immersed in either the mixed PAZO+DR80 solution or the pure DR80 solution for five minutes at room temperature, rinsed, and dried as before. This method resulted in a single bilayer of PEI/(DR80+PAZO) or PEI/DR80. Depending on the experiment, up to 10 bilayer films were constructed.

(18) Reveda, T.; Petkanchin, I. *J. Colloid Interface Sci.* **1997**, *196*, 87.

(19) Johal, M. S.; Ozer, B. H.; Casson, J. L.; St. John, A.; Robinson, J. M.; Wang, H. L. *Langmuir* **2004**, *20*, 2792.

Spin-assembled films were constructed at room temperature on a Headway Research photoresist spinner at 3000 rpm. The spin-assembly process consisted of pipetting PEI solution (1 mL) onto a spinning substrate and spinning for 1 min. The substrate was then placed in an ambient 110 °C environment for 1 min and then cooled in air for 1 min. The PAZO+DR80 (or DR80) solution (1 mL) was then deposited onto the spinning film surface and spun for 1 min. The drying procedure was repeated as before. The deposition of PEI and PAZO+DR80 (or DR80) layers was repeated until a multilayered film with the desired number of bilayers was constructed.

UV–visible measurements of the multilayered films built on glass substrates were taken between 280 and 700 nm on a Varian Cary 300 spectrophotometer. Spectra were obtained for every bilayer. Thickness measurements were collected by single-wavelength null ellipsometry using a Rudolph Technologies AutoEL III and a Rudolph Instruments model 439L633P ellipsometer. Data were collected at a beam incidence angle of 70° and a wavelength of 632.8 nm. A refractive index of $1.5 \pm 0i$ was used to manually calculate ellipsometric film thickness from Δ and Ψ parameters. The thickness of the native oxide layer on Si was determined for every substrate used. This value was then subtracted from the film measurements to determine actual ellipsometric film thickness.

Results and Discussion

The bulk aqueous phase solution spectrum of PAZO shows a maximum absorbance at $\lambda_{\max} = 353$ nm, corresponding to the π – π^* transition of the azobenzene group. When assembled in ESA and spin-assembled films, this absorption peak is red-shifted to $\lambda_{\max} = 363$ nm. The shift is likely due to the presence of noncovalent interactions, or chromophore-coupling effects,²⁰ between the azo-benzene chromophores in the aggregated system. Such effects for PAZO are believed to occur through the mode of J-aggregation, in which chromophores are aligned in a “head-to-tail” arrangement.²¹ DR80, in contrast, shows bulk phase absorbances (a doublet at $\lambda_{\max} = \sim 525$ and ~ 555 nm) not significantly shifted from the values obtained for ESA and spin-assembled films.

Figure 2a shows the UV–visible absorbance at λ_{\max} for 10 bilayers of PEI/DR80 both for spin-assembled films and films constructed using ESA. The spin-assembled film is deposited on a single side of the substrate, compared to the double-sided ESA film. The absorbance values at $\lambda_{\max} = 550$ nm suggest that a significantly greater amount of DR80 deposits in the ESA film than in the spin-assembled film. Ellipsometry results in Figure 2b show a similar picture, with a single-side thickness for the ESA film (225 Å) more than twice that of the spin-assembled film (87 Å). Given the entanglement adsorption mechanism and the short liquid-substrate contact time in spin-assembly, one would expect a lower deposition amount of DR80 in spin-assembled films compared to ESA for the same solution concentrations. We can also compare the ratios between single-side thickness and single-side UV–visible absorbance for both of our films to obtain a comparison of overall density. The numerical results of ~ 1050 and ~ 1400 Å per absorbance unit, calculated for the ESA and spin-assembled films, respec-

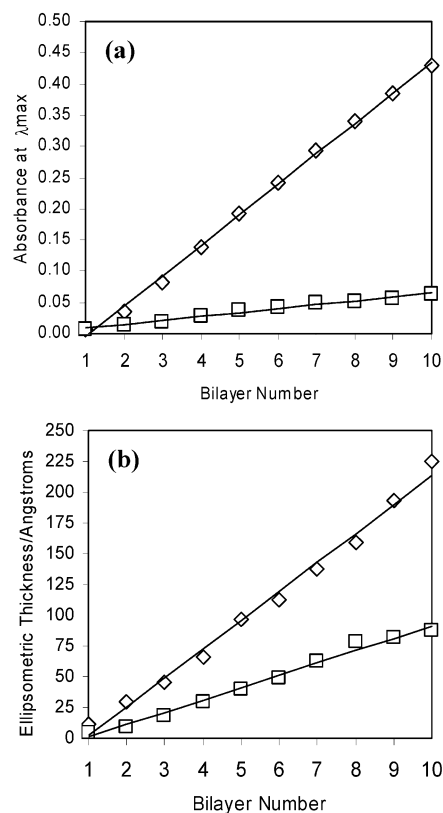


Figure 2. (a) UV–visible absorbance at λ_{\max} (~ 550 nm) for the PEI/DR80 system as a function of bilayer number. Multilayered films were constructed using both ESA (\diamond), and spin-assembly (\square). (b) Ellipsometric thicknesses for the PEI/DR80 system as a function of bilayer number. Multilayered films were constructed using both ESA (\diamond), and spin-assembly (\square).

tively, demonstrate that spin-assembly generates a less-dense packing structure of the DR80 layer. Such a reduction in packing density could result from greater interpenetration of DR80 into the PEI layer, or could be due to reduced coherent alignment of the DR80 molecules themselves, yielding a layer with empty space between irregularly stacked subunits.

Mixed solution deposition of the type PEI/(DR80+PAZO) was used to build both spin-assembled and ESA multilayered films. Figure 3 shows UV–visible spectra of 10 bilayers of PEI/(DR80+PAZO) for both types of films. The presence of an absorption band at ~ 360 and ~ 550 nm in both spectra indicates the presence of DR80 and PAZO in the multilayered films. However, the relative amount of adsorbed PAZO compared to DR80 is significantly greater in the spin-assembled film ($\sim 1:0.4$) than in the ESA film ($\sim 1:1.5$). We see that our choice of assembly technique may directly influence the molecular composition of a mixed layer. This observation demonstrates the utility of spin-assembly as a method for building layered structures otherwise unattainable by ESA. The deposition of more PAZO than DR80 in spin-assembled films supports our previous hypothesis that entanglement of molecular chains may contribute significantly to the spin-assembly process.^{10,13,15} If we compare the amount of DR80 in the PEI/(DR80+PAZO) structure with the amount in the PEI/DR80 films, we see that the addition of PAZO reduces the amount of DR80 adsorbed by approximately half, when using both spin-assembly and ESA. Notably, such an effect occurs despite the unequal ratios

(20) Kuhn, H.; Kuhn, C. Chromophore Coupling Effects. In *J-Aggregates*; Kobayashi, T., Ed.; World Scientific: Singapore, 1996; pp 1–40.

(21) Dante, S.; Advincula, R.; Frank, C. W.; Stroeve, P. *Langmuir* **1999**, *15*, 193.

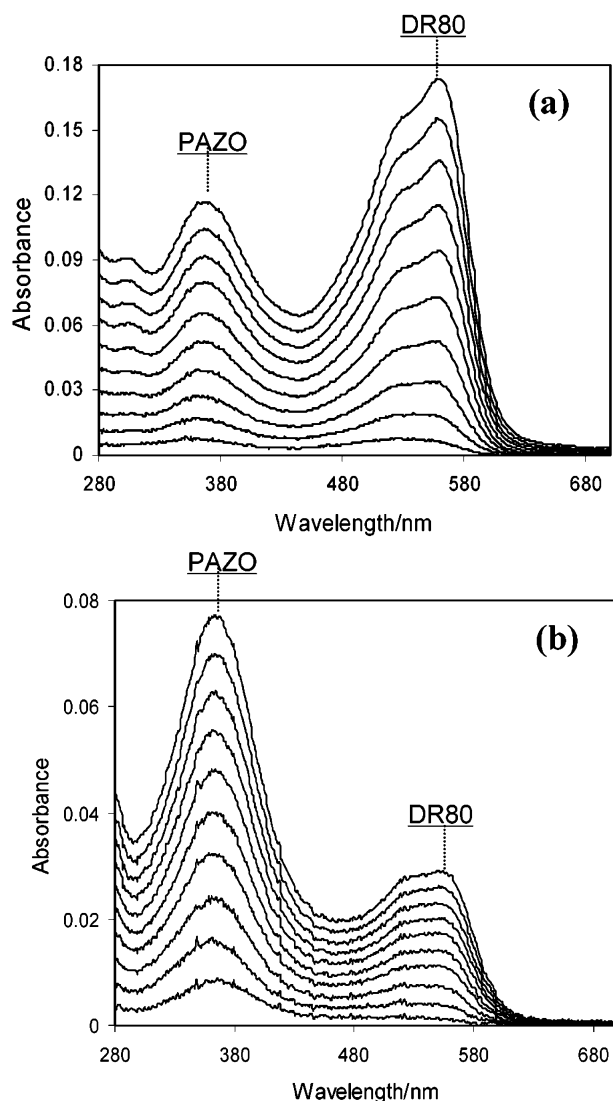


Figure 3. UV-visible absorbance spectra of the PEI/(DR80+PAZO) system as a function of bilayer number. Multilayered films were constructed using both ESA (a), and spin-assembly (b).

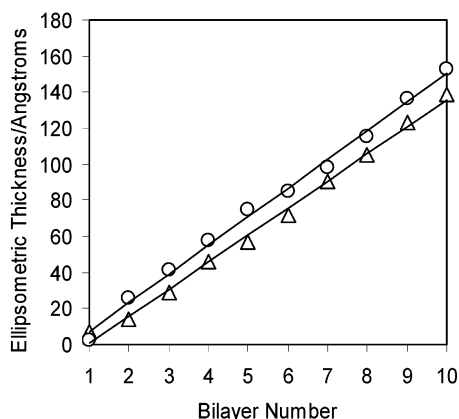


Figure 4. Ellipsometric thicknesses for the PEI/(DR80+PAZO) system as a function of bilayer number. Multilayered films were constructed using both ESA (Δ), and spin-assembly (\circ).

between PAZO and DR80 in each case. Figure 4 shows the ellipsometric thickness values of the PEI/(DR80+PAZO) system for both types of films. Even though the two assembly methods deposit different amounts of DR80 and PAZO, the spin-assembled PEI/(DR80+PAZO) film is of thickness

Table 1. Absorbance Values and Ellipsometric Thicknesses of ESA and Spin-Assembled Films Comprised of 10 Bilayers

film	absorbance ^a	thickness/ \AA
ESA (PEI/DR80) ₁₀	0.214 (~540 nm)	225
Spun (PEI/DR80) ₁₀	0.062 (~540 nm)	87
ESA (PEI/DR80+PAZO) ₁₀	0.058 (~360 nm), 0.086 (~540 nm)	139
Spun (PEI/DR80+PAZO) ₁₀	0.076 (~360 nm), 0.028 (~540 nm)	153
ESA (PEI/PAZO) ₁₀	0.165 (~360 nm)	400
Spun (PEI/PAZO) ₁₀	0.138 (~360 nm)	150

^a Absorbances of ESA films have been halved for comparison.

comparable to that of the PEI/(DR80+PAZO) ESA film. Comparing with the PEI/DR80 films once again, we see that the spin-assembled PEI/(DR80+PAZO) system yields films of greater thickness than the spin-assembled PEI/DR80 system, while the effect is the opposite for the ESA system. In the case of ESA, the equilibrium-state adsorption of PAZO close to the substrate, while the rapid process of spin-assembly may deposit PAZO in a higher-energy coiled conformation.

We observe that the λ_{max} values of PAZO and DR80 in the coadsorbed films are identical to the corresponding λ_{max} values of each substance in the pure bilayer films (PEI/PAZO and PEI/DR80). The lack of peak shifting suggests that there may be minimal π - π interaction between PAZO and DR80 in the coadsorbed film, which commonly arises from preferential molecular aggregation.²¹

Table 1 lists film thickness and absorbance values for the tenth bilayer of ESA and spin-assembled films. The absorbance values for the ESA films have been divided by a factor of 2, representing the amount present on a single side. As previously noted, the spin-assembled PEI/DR80 film has the smallest ellipsometric thickness (87 \AA), reflecting the difficulty of assembling thick layers from monomeric molecules. Ten bilayers of the spin-assembled PEI/(DR80+PAZO) system give thickness comparable to that of a spin-assembled PEI/PAZO system (~ 150 \AA) constructed in previous work.¹⁰ Comparing film thickness to PAZO UV-visible absorbance amounts, we observe a PAZO density in the spin-assembled PEI/PAZO film approximately *twice* that of the spin-assembled PEI(PAZO+DR80) film (~ 1080 and ~ 2010 \AA /absorbance unit, respectively). Corresponding mixed composition ESA films (139 \AA) are much thinner than ESA PEI/PAZO films (400 \AA), although a similar comparison of absorbance and ellipsometric thickness shows that PAZO density is almost equal in these films (~ 2420 and ~ 2400 \AA /absorbance unit). Our observations here suggest that the structure of mixed films deposited using ESA may be dominated by the polymeric species in the film. When such a system is allowed to reach equilibrium, the optimal PAZO density is reached, despite the presence of DR80. We take this observation as further evidence to the noninteracting nature of the two species. In spin-assembled films, physisorption must occur on a very rapid time-scale, effectively halting deposition at a point prior to equilibrium. Under such conditions, we see that PAZO density may be effectively altered simply by the presence of an additional species. This disparity in density appears to be present only for the PAZO

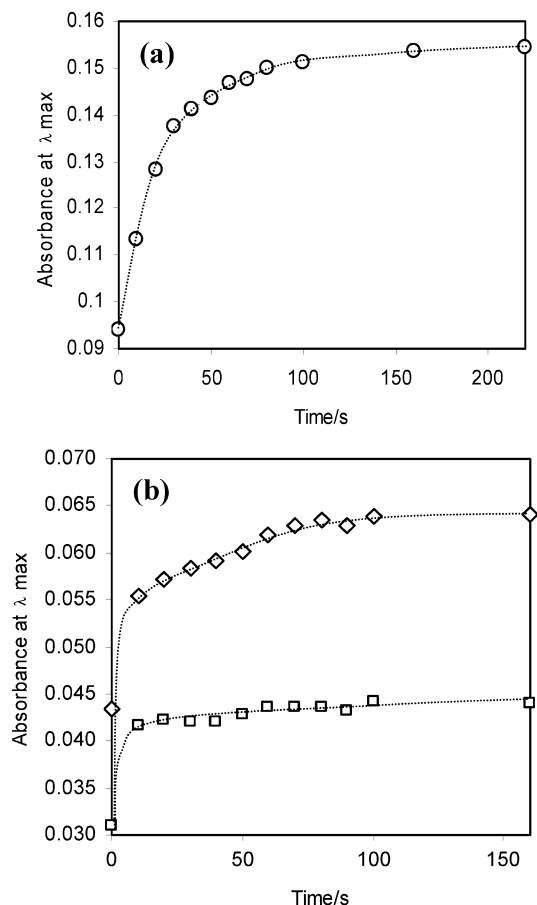


Figure 5. Kinetics of adsorption for ESA films. (a) Absorbance at 550 nm as a function of DR80 adsorption time, in a PEI/DR80 system. (b) Absorbance at 550 nm (\diamond) and 360 nm (\square) as a function of (DR80+PAZO) adsorption time, in a PEI/(DR80+PAZO) system. In both (a) and (b), kinetic measurements were taken after constructing four bilayers.

component of the mixed bilayer. DR80 density decreases substantially in PEI/(PAZO+DR80) films compared to PEI/DR80 films, using both methods for assembly. In estimating density, we make the assumption that PAZO and DR80 are well mixed throughout the layer profile, rather than segregated to a specific portion of the layer. Furthermore, we make the assumption, based on prior work, that the films possess a high degree of interpenetration.^{3,14,19} Despite these assumptions the approach for estimating chromophore density is instructive. Upcoming work will employ more stringent methods for density estimation.

Kinetics of DR80 adsorption on PEI using ESA was monitored by UV–visible spectroscopy. Figure 5a shows the time-halted maximum absorbance of DR80 from 0 to 220 s, obtained by removing the substrate from solution, quickly rinsing it, and drying it with N_2 at specified intervals during deposition. To minimize any substrate influence,¹³ these measurements were obtained at the fifth DR80 layer after constructing four PEI/DR80 bilayers terminating with PEI. As seen in Figure 5, the time taken for the fifth DR80 layer to reach saturation coverage is approximately 100 s. We calculate ~ 70 s as the time to 95% of maximum

absorbance. Maximum adsorption of DR80 occurs within the 5 min allotted for each adsorption cycle of the multi-layered film, providing confirmation that our ESA deposition scheme allows the system to reach equilibrium.

Kinetics of DR80 and PAZO coadsorption on PEI was also monitored by UV–visible spectroscopy in a manner similar to that used for the PEI/DR80 layers. Figure 5b shows the time-halted absorbance at 360 and 550 nm from 0 to 160 s. In the presence of PAZO, Figure 5b shows that DR80 adsorption is more rapid than when DR80 adsorbs alone, reaching 95% of the estimated maximum value at ~ 52 s compared to the previous ~ 70 s. Even more striking is the fast PAZO adsorption in this film, which appears to reach saturation prior to the competing DR80. We see that PAZO reaches 95% of maximum within ~ 20 s, compared to the corresponding value of 260 s in a PEI/PAZO system.¹⁴ Although we observe this change in the rate of PAZO adsorption, the resulting systems have similar PAZO densities, as described previously. This result suggests that the addition of a small molecule to an adsorbing mixture may enhance the rate of film formation, with minimal impact on the distribution of the polymeric species of interest.

Summary

We have successfully integrated the dye molecule DR80 into electrostatic self-assembled films, both with DR80 as the sole component of an anionic layer, and with DR80 coadsorbed from a mixture containing the polyanion PAZO. Furthermore, we have demonstrated for the first time that spin-assembly can be used to accomplish both of these deposition schemes. Our results widen the range of applications for the spin-assembly technique, which is rapidly becoming a popular method of thin film formation.^{22–26} We found that the adsorption of pure DR80 layers on a PEI surface is significantly influenced by the deposition process chosen, with layers of lower packing density constructed by spin-assembly, compared to ESA. Coadsorption of DR80 and PAZO on a PEI surface may be influenced to occur in specific proportions and packing densities, depending on the assembly technique selected. We found that using DR80 as a coadsorbing agent can dramatically enhance the rate of PAZO adsorption, and we observed different deposition rates for DR80 and PAZO when the two materials adsorb simultaneously from a common solution. Our results here demonstrate significant progress in attaining directed control of self-assembled multilayers.

Acknowledgment. This work was supported by the New College Division of Natural Sciences, the Camille and Henry Dreyfus Foundation, and the New College Foundation.

CM048905P

- (22) Jiang, C.; Markutsya, S.; Tsukruk, V. V. *Langmuir* **2004**, *20*, 882.
 (23) Pinto, M. R.; Kristal, B. M.; Schanze, K. S. *Langmuir* **2003**, *19*, 6523.
 (24) Jang, H.; Kim, S.; Char, K. *Langmuir* **2003**, *19*, 3094.
 (25) Sohn, B.-H.; Kim, T. H.; Char, K. *Langmuir* **2002**, *18*, 7770.
 (26) Jiang, C.; Markutsya, S.; Tsukruk, V. V. *Adv. Mater* **2004**, *16*, 157.